



Submitted: 15.12.2021
Accepted: 21.01.2022
Early publication date: 13.04.2022

Endokrynologia Polska
DOI: 10.5603/EPa2022.0011
ISSN 0423-104X, e-ISSN 2299-8306
Volume/Tom 73; Number/Numer 2/2022

Astragaloside IV drug-loaded exosomes (AS-IV EXOs) derived from endothelial progenitor cells improve the viability and tube formation in high-glucose impaired human endothelial cells by promoting miR-214 expression

Xiaoling Zou¹, Hui Xiao¹, Xue Bai¹, Yixian Zou¹, Wenxiao Hu¹, Xiangdong Lin¹, Chenhong Zhu², Yao Liang², Wu Xiong³

¹Department of Endocrinology, the First Affiliated Hospital of Hunan University of Chinese Medicine, Changsha, Hunan, China

²College of Integrated Traditional Chinese and Western Medicine, Hunan University of Chinese Medicine, Changsha, Hunan, China

³Department of Burns and Plastic Surgery, the First Affiliated Hospital of Hunan University of Chinese Medicine, Changsha, Hunan, China

Abstract

Introduction: The high glucose changes caused by diabetes mellitus (DM) can damage the vascular system. Astragaloside IV (AS-IV) can improve diabetes and promote angiogenesis. Exosomes (EXOs) help to carry specific drugs into cells efficiently. However, whether AS-IV loaded EXOs (AS-IV EXOs) can improve damaged endothelial cells through miR-214 remains to be determined.

Material and methods: We prepared and identified AS-IV EXOs derived from endothelial progenitor cells (EPCs) and high glucose stimulated endothelial cell models to investigate whether AS-IV EXOs can improve damaged endothelial cells through miR-214. We used a transmission electron microscope (TEM) and DAPI staining to identify the morphology and characteristic expression of EPCs and EXOs, and then prepared AS-IV EXOs. Cell function tests were performed to detect the cloning, proliferation, and migration capabilities of cells. Western blot (WB) and real-time quantitative polymerase chain reaction (qRT-PCR) were used to assess the expression level of Tie-2, Ang-1, and PI3K/Akt-related protein.

Results: The DAPI staining results showed that inducing human umbilical vein endothelial cells (HUVECs) could effectively absorb AS-IV EXOs. The results of plate clone formation assay, CCK-8, cell adhesion, and transwell assay of HUVECs stimulated by high glucose showed that AS-IV EXOs had a damage relief effect. By the detection of WB and qRT-PCR, it was found that AS-IV EXOs promoted the expression of miR-214 and proteins related to blood vessel growth. After transfection of miR-214 to pre-treat HUVECs under high glucose stimulation, AS-IV EXOs promoted the tube formation of HUVECs by regulating the level of miR-214.

Conclusions: By promoting the expression of miR-214, AS-IV EXOs significantly improved the activity and tubularization of HUVECs under high glucose stimulation. (*Endokrynol Pol* 2022; 73 (2): 336–345)

Key words: astragaloside IV; endothelial cells; miR-214; exosomes; tube formation; diabetes mellitus

Introduction

Diabetes mellitus (DM) is a multifactorial metabolic disease caused by a deficiency of insulin secretion or utilization [1, 2]. As one of the world's fastest growing diseases, it is expected to affect 693 million adults by 2045 [3]. Cardiovascular and microvascular complications associated with the vascular system comprise the main cause of morbidity and mortality in patients with diabetes [4]. Excessive blood sugar levels can damage the integrity of the endothelial layer, leading to delayed re-endothelialization and excessive formation of new intima [5]. It also leads to metabolic disorders and oxidative stress of cardiovascular epithelial cells, resulting in increased permeability, impaired endothelial relaxation,

decreased NO content, and other effects, increasing the risk of heart failure [6]. Therefore, inducing human umbilical vein endothelial cells (HUVECs) to improve their biological function through drugs or physical therapy will help to improve the vascular complications of diabetes.

AS-IV is isolated and purified from the Chinese herbal medicine astragaloside, and it has antioxidant, anti-diabetes, anti-myocardial infarction, anti-inflammatory, and anti-apoptosis effects, and promotes angiogenesis [7]. Nie et al. showed that AS-IV significantly improved endothelial dysfunction, decreased oxidative stress and calpain-1 content, and increased nitric oxide (NO) production and expression of endothelial nitric oxide synthase (eNOS) in the thoracic aorta of diabetic rats [8]. Leng et al. found that AS-IV rescued endothelial



Wu Xiong; The First Affiliated Hospital of Hunan University of Chinese Medicine, No.95, Middle Shaoshan Road, Yuhua District, Changsha City, Hunan Province, China; e-mail: kkkytd3326@126.com

dysfunction induced by high glucose by inhibiting the P2X7R-dependent P38 MAPK signalling pathway [9]. However, there are few studies on the treatment of DM with AS-IV in the form of nanospheres.

EXOs are biological extracellular vesicles with a size between 50 and 150 nm, which are secreted by cells and isolated from body fluids [10]. Extracellular vesicles can bypass biological barriers and act as powerful drug and gene therapy transporters [11]. EXOs have certain biological regulatory functions. For example, EXOs secreted by cardiac progenitor cells (CPC) can reduce the apoptosis of cardiac cells, promote angiogenesis, and improve the degree of heart damage [12]. IVPCs-EXOs secreted by induced vascular progenitor cells (iVPCs) can promote endothelial cell proliferation, migration, and angiogenesis, and stimulate microangiogenesis *in vitro* aortic ring test [13]. Moreover, due to the physical properties of EXOs such as stability, biocompatibility, permeability, low toxicity, and low immunogenicity, in addition to being used as disease biomarkers, they are also used as endogenous natural carriers to deliver chemotherapeutic drugs [14].

miR-RNAs are a type of small single-stranded non-coding RNA, usually about 22 bp, which regulate gene expression after transcription [15]. Among them, miR-214 is associated with inflammation, myocardial injury, endothelial cell angiogenesis, and apoptosis. miR-214 may reduce urea-induced apoptosis of mouse aorta endothelial cells (MAEC) by inhibiting COX-2/PGE2 cascade reaction [16]. miR-214 may antagonize endothelial cell apoptosis induced by indoxyl sulphate (IS) by directly down-regulating the COX-2/PGE₂ axis and targeting COX-2 [17]. Chondrocyte miR-214-3p promotes endothelial cell angiogenesis and migration by adjusting the secretion of vascular endothelial growth factor (VEGF) through the Trkb/ShcB pathway [18]. However, it is still unknown whether miR-214 is involved in the regulation of endothelial cell apoptosis.

Based on the above background, we prepared AS-IV EXOs derived from endothelial progenitor cells (EPCs) and created a model of endothelial cell damage with high glucose. Then we conducted *in vitro* cell and molecular experiments. The purpose of this study was to clarify whether AS-IV EXOs can improve the activity and angiogenesis of human endothelial cells damaged by high glucose by promoting the expression of miR-214.

Material and methods

Separation and identification of EPCs

Under aseptic conditions, cord blood EPCs were extracted from the placental cord blood of normal caesarean section in the First Affiliated Hospital of Hunan University of Traditional Chinese Medicine (all participants signed informed consent forms, and the study was approved by the Ethics Committee of our hospital, No.

HN-LL-KY-2020-013-01). Umbilical cord blood mononuclear cells were separated by density gradient centrifugation. The cells were cultured in EGM-2 complete medium (CC-3162, LONZA company). When the cell fusion rate reaches 70-80%, the cells were digested with 0.25% pancreatin (containing 0.02% EDTA). The cells were centrifuged at 1000 rpm for 5 min, and the pellet was redispersed in EGM-2 complete medium and subcultured in a ratio of 1:2 or 1:3. The cell morphology of EPC was observed under a light microscope. The CD31 immunomagnetic bead sorting method and the FITC-UEA-I and Dil-ac-LDL dual fluorescence staining method were used to identify the P3 generation cells in good growth condition. The cells were inoculated into a 24-well plate with pre-placed slides and cultured overnight. The cells were washed 3 times with PBS. 250 μ L of culture solution containing Dil-ac-LDL (10 μ g/mL) was added to the cell liquid in the dark. Cells were incubated in a 37°C, 5% CO₂ incubator for 4 hours. After the incubation, the culture medium was aspirated and washed with PBS 3 times, and 4% paraformaldehyde was added for fixation for 30 min. After washing the cells 3 times, 250 μ L of FITC-UEA-1 (10 μ g/mL) was added to the cell liquid for 1 hour in the dark. After washing the cells 3 times, 250 μ L of DAPI working solution (1 μ g/mL) was added to the cell liquid at 37°C. Images were collected after 10-min incubation in the dark.

Separation and identification of EXOs

According to the instructions of the EXOs extraction kit (EXOQ5A-1, SBI), EXOs secreted by EPCs in the early culture stage (P3 generation) were extracted. After the EPC cell supernatant was collected, the cells and cell debris were discarded following centrifugation for 10 min. After the supernatant was moved to a new centrifuge tube, the EXOs extraction reagent was added in a volume ratio of the cell supernatant as follows: EXOQ5A-1 = 5:1. After the cells were allowed to stand overnight at 4°C, the cell solution was centrifuged at 1500 g to obtain the EXOs pellet, and then 100 μ L of PBS was added to resuspend the pellet.

Transmission electron microscope (TEM)

The 10 μ L EXOs suspension was sucked onto the copper mesh with a membrane and allowed to stand at room temperature for 1–5 min. After the filter paper absorbed the excess EXOs sample on the copper mesh, 10 μ L of phosphotungstic acid staining solution (prepared with phosphoric acid buffer to a concentration of about 1%) was dripped onto the copper mesh of the prepared sample. After standing for 1–2 min, the excess dye was removed. Pure water was dripped on the copper net several times to wash away the excess phosphotungstic acid. After the copper mesh was allowed to stand and dry, a transmission electron microscope was applied to observe the EXOs morphology.

Nanoparticle tracking analysis (NTA)

The information on particle size, concentration, and distribution can be provided by NTA performed by a Particle Metrix instrument. A NanoSight NS300 was used to detect EXOs under the condition of 405 nm, and 5 videos of 60 s duration were collected for each sample. The data were analysed by NTA 3.0 software, and the fluid dynamic diameter of each EXOs was calculated by the Stokes-Einstein equation.

Detection of AS-IV EXOs uptake by HUVECs

PKH67 dye-labelled EXOs was centrifuged at 1500 g for 0.5 h, and the pellet was redispersed in 500 μ L PBS. The resuspension was transferred to a 10 KD ultrafiltration tube and centrifuged at 3000 g for 40 min. The collected and concentrated EXOs were resuspended and diluted to 500 μ L in DMEM high sugar with 10% FBS, and then added to a 12-well plate of HUVECs cells (ATCC, Manassas, VA, USA) pre-placed with slides. The slides were cultured in a 37°C, 5% CO₂ incubator for 24 hours. The slides were taken out and washed twice with PBS, and then fixed with 4% paraformaldehyde (Wellbio, Changsha, China) for 0.5 h. The slides were cultivated with 1

$\mu\text{g/mL}$ DAPI at 37°C in the dark for 10 min and washed with PBS 3 times. The results were observed using a fluorescence microscope (BA410T, MOTIC, Singapore).

Cell culture and treatment

The endothelial cells were grown to 80% in the culture flask and cultured in DMEM medium with 30 mmol/L glucose for 5 days to obtain high-glucose-damaged endothelial cells. The morphology of endothelial cells damaged by high glucose was observed under an optical microscope. To study the mitigation effect of AS-IV EXOs on HUVECs damages under high glucose stimulation, the endothelial cells injured by high glucose were divided into 4 groups: a blank group (high-glucose-damage endothelial cells), an experimental group (100 μg AS-IV EXOs), an AS-IV group (HUVECs mediated with 100 mg/L AS-IV), and an EXOs group (EPC-EXOs with PBS intervention). After 48 hours, the sampling observation results were processed.

Cell transfection

In order to study the relationship between the effect of AS-IV EXOs on HUVECs and the change of miR-214 level, the successfully identified high-glucose-damaged endothelial cells were divided into 6 groups: an NC-inhibitor group, an miR-214 inhibitor group, an NC-mimic group, an miR-214 mimic group, an AS-IV EXOs + miR-214 inhibitor group, and an AS-IV EXOs + miR-214 mimic group. After 48 hours, the sampling observation results were processed. HUVECs in the NC-inhibitor group were transfected with NC inhibitor. HUVECs in the miR-214 inhibitor group were transfected with miR-214 inhibitor. HUVECs in the NC-mimic group were transfected with NC-mimic. HUVECs in the miR-214 mimic group were transfected with miR-214 mimic. HUVECs in the AS-IV EXOs + miR-214 inhibitor group were transfected with miR-214 inhibitor and cultured with AS-IV EXOs. HUVECs in the AS-IV EXOs + miR-214 mimic group were transfected with miR-214 mimic and cultured with AS-IV EXOs. After 48 hours, the sampling observation results were processed.

Plate clone formation assay

After the cells were inoculated in 6-well plates, they were cultured in an incubator at 37°C for 3 days. The culture medium was scattered, and the cells were rinsed twice with PBS. The cells were fixed with 4% paraformaldehyde for 0.5 h and then rinsed with PBS and stained with 0.5% crystal violet for 5 min. After the excess staining solution was washed away, each hole was photographed in the camera, and the number of clones was counted.

Ethylene diurea (EDU)

The cells were digested with 0.25% trypsin, and resuspended in complete medium to make a single cell suspension. 2×10^5 cells were inoculated into each well of a 96-well plate, and 50 μL of 50 μM EDU medium was added and incubated for 24 hours. The cells were rinsed with PBS and fixed with 4% paraformaldehyde for 0.5 h. The cells were dispersed with 2 mg/mL glycine for 5 min and then rinsed with PBS. 100 μL of penetrant decolorization was added to the cells in each well and incubated for 10 min. After washing the cells, 100 μL of 1 \times Apollo® staining reaction solution was added to the cells and incubated for 30 min. After 100 μL penetrant was added, it was washed with 100 μL methanol and PBS in turn. Each well was added with 100 μL 1 \times Hoechst 33342 reaction solution and incubated for 30 min. After washing with 100 μL PBS 3 times, the fluorescence signal intensity was detected by a microplate reader. The fluorescence signal intensity was directly proportional to the cell proliferation ability.

Cell Counting Kit-8 (CCK-8)

Cells were digested with trypsin digestion solution to prepare cell suspension. $1 \times 10^4/100 \mu\text{L}$ cells were seeded in 96-well plates. After

the cells were cultured overnight, they were treated with different interventions according to experimental groups. After culturing for 1 hour, the culture medium was aspirated and dispersed with 110 μL CCK-8 working solution (100 μL medium + 10 μL CCK-8 mother solution). The cells were cultured in a 37°C incubator for 4 hours, and the absorbance value at 450 nm was measured by a microplate reader.

Trypan blue staining

The trypan blue staining method was used to detect the viability of endothelial cells under high glucose injury. The cells were digested with trypsin digestion solution, and the collected cells were centrifuged at 1000–2000 g for 1 min. The cells were dispersed in the cell resuspension solution. 100 μL of the resuspended cells was pipetted into a centrifuge tube and stained with 100 μL trypan blue staining solution. After 3 min of incubating, the number of cells was counted by a haemocytometer.

Cell adhesion

The prepared cell suspension was seeded in a 96-well plate according to $1 \times 10^4/100 \mu\text{L}$. After culturing for 30 min, the cells were rinsed 3 times with serum-free DMEM to remove non-adherent cells. The cells were replaced with 100 μL serum-free medium, and 10 μL CCK-8 solution was added to each well. The cells were incubated at 37°C for 4 hours, and the absorbance at 450 nm was measured by a microplate reader. The absorbance value is positively correlated with the number of cell adhesion.

Transwell assay

The cells were digested with 0.25% trypsin digestion solution. The cells were prepared into a cell suspension with serum-free basal medium, and the cell density was adjusted to about $1 \times 10^5/\text{mL}$. 100 μL of cell suspension was added to the upper chamber of the small chamber, and the lower chamber was filled with complete medium containing 10% FBS. After the cells were cultured for 48 hours, they were washed twice with PBS. The cells on the upper chamber surface were wiped off with a wet cotton swab and fixed with an equal mixture of acetone and methanol for 20 min. The cells were washed with PBS and stained with 0.5% crystal violet for 5 min, and then washed with water more than 3 times. Cell migration was observed under an inverted microscope.

Endothelial tube formation assay

The cells were digested with 0.25% trypsin (with 0.02% EDTA) and dispersed evenly. The cell suspension was centrifuged at 1000 rpm for 5 min, and then were resuspended in basic complete medium. Cells were seeded into 6-well plates at $2 \times 10^5/\text{well}$ and cultured overnight. According to the cell grouping, the corresponding experimental intervention treatment was carried out. 200 μL Matrigel was added to each well of the 48-well plate to cover the wells evenly, and the 48-well plate was placed in a 37°C incubator for 1 h. The above-mentioned interventional cells were digested with 0.25% pancreatin (containing 0.02% EDTA) to prepare a cell suspension. According to the experimental groups, the culture medium was used to make a 7.5×10^4 cells/well cell suspension, and then added to the 48-well plate. The result was observed after 6 hours of incubation at 37°C .

Western blot (WB)

The cells were washed once with ice-cold PBS and centrifuged at 3000 rpm for 2 min. 100 μL of RIPA lysate was added to the cells and sonicated for 1.5 min. Ice-cold PBS was added to wash the cells once. 200 μL of RIPA lysate was added and the cells were scraped off with a cell scraper. The suspension was sonicated for 1.5 min, lysed on ice for 10 min, and centrifuged at 12,000 rpm at 4°C for 15 min. The supernatant after centrifugation was transferred to a 1.5 mL centrifuge tube. The protein content was detected by the BCA method.

5× loading buffer was added to the solution in a 4:1 ratio and denatured at 100°C for 5 min. SDS-PAGE was electrophoresed at 75 V for 130 min and then transferred to the membrane at 300 mA for 1 h. After 5 min of TBST rinsing, 5% skimmed milk was blocked for 1.5 hours, TBST was rinsed for 15 min, and CD63(25682-1-AP, 1:300, proteintech, USA), CD81 (66866-1-Ig, 1:3000, proteintech, USA), CD9 (20597-1-AP, 1:300, proteintech, USA), GAPDH(60004-1-Ig, 1:5000, proteintech, USA), PI3K (67071-1-Ig, 1:5000, proteintech, USA), p-Akt(66444-1-Ig, 1:5000, proteintech, USA), Ang-1 (ab183701, 1:10000, abcam, UK), Tie-2(19157-1-AP, 1:500, proteintech, USA), and β -actin (60008-1-Ig, 1:5000, proteintech, USA) primary antibodies were added and incubated overnight at 4°C. The PVDF membrane was taken out and rinsed with TBST. The secondary antibody HRP goat anti-mouse IgG (SA00001-1, 1:5000, Proteintech, USA) or HRP goat anti-rabbit IgG (SA00001-2, 1:6000, Proteintech, USA) was added, incubated at 25°C for 1.5 h, and rinsed with TBST. The Western strip image was scanned and analysed by a chemiluminescence imaging system (Guangzhou Qinxiang Company). GAPDH or β -actin was used as an internal control.

Quantitative real-time polymerase chain reaction (qRT-PCR)

The TRIzol method was used to extract total RNA from cells and tissues, and an mRNA reverse transcription kit (CW2569, Kangwei Century, Beijing, China) was applied to reverse transcription cDNA. The primer sequences of ANG-1, PI3K, Akt, TIE-2, U6, hsa-miR-214-5p, and β -actin were designed and synthesized by Sangon Biotech (Tab. 1). Fluorescent dyes were added to prepare the qRT-PCR reaction system. A 20 μ L reaction system was used for the detection of the qRT-PCR amplification program. The reaction conditions were as follows: 95°C pre-denaturation for 10 min; 95°C denaturation for 15 seconds, 60°C annealing for 30 seconds, 40 cycles; melting curve analysis at 60–95°C. DNA amplification and real-time monitoring of fluorescence signals were carried out by a fluorescence quantitative PCR instrument (PIKOREAL96, Thermo, USA) to obtain each gene's amplification curve and melting curve. U6 and β -actin were used as internal controls, and the relative expression of genes in each sample was calculated using the $2^{-\Delta\Delta Ct}$ method.

Table 1. Primers used in this study

Primer ID	5'-3'
β -actin-F	ACCCTGAAGTACCCATCGAG
β -actin-R	AGCACAGCCTGGATAGCAAC
Ang-1-F	AAGCCGTAACATGAACCTCTCG
Ang-1-R	TTCCCTGTATCTTGTGGCCAT
PI3K-F	TGCGTCTACTAAAATGCATGG
PI3K-R	AACTGAAGGTTAATGGGTCA
Akt-F	AGCCCTGGACTACCTGCACTCG
Akt-R	CTGTGATCTTAATGTGCCCGTCCT
Tie-2-F	TGCTTGGACCCTTAGTGA
Tie-2-R	TTGAACCTTGTAACGGATAG
U6-F	CTCGCTTCGGCAGCACA
U6-R	AACGCTTACGAATTTGCGT
hsa-miR-214-5p-F	TGCCTGTCTACACTTGCTGTGC
hsa-miR-214-5p-R	GCTGTCAACGATACGCTACGTAA

Statistical analysis

SPSS 20.0 (SPSS Inc) was used for statistical analysis. The data are represented as the mean \pm standard deviation ($\bar{X} \pm SD$). Student's t-test was used to analyse the differences between 2 groups, and one-way analysis of variance (ANOVA) was used to compare the data differences between multiple groups. $P < 0.05$ was considered statistically significant.

Results

Absorption of AS-IV EXOs by HUVECs

The EPCs after centrifugation and culture were observed and identified under a light microscope. The results are shown in Figure 1A; the cells present a typical colony morphology, with the central cells in a round shape and the peripheral cells in a spindle shape. The results of identifying human EPCs by fluorescence method are shown in Figure 1B, the fusion image showed that the cells with orange-yellow membrane changes were normally differentiated EPCs. In order to observe the morphological structure of EXOs collected from the supernatant of EPC cells, a cup-shaped vesicle-like structure with a diameter of about 40–150 nm was observed under a TEM electron microscope (Fig. 1C). The NTA results are shown in Figure 1D, and the EXOs size reached a peak value of 56–132 nm. WB was used to assess the expression of EXOs-related proteins. The results are shown in Figure 1E. Three EXOs marker proteins, CD9, CD63, and CD81, were detected in each group, and the difference was not statistically significant ($p > 0.05$). This illustrated that EPCs and EXOs were successfully separated. The fusion image showed that HUVECs could effectively take up AS-IV EXOs (Fig. 1F).

The effect of AS-IV EXOs on cell viability and tube formation of HUVECs damaged by high glucose

According to the results shown in Figure 2A, compared with the blank group, the number of cell clones in the AS-IV EXOs group was significantly increased ($p < 0.05$), and the number of cell clones in the EXOs group was also higher than that in the blank group ($p < 0.05$). At the same time, compared with the EXOs group, the AS-IV group also showed an increased number of cell clones. According to Figure 2B, compared with the blank group, the apoptosis rate of the AS-IV EXOs group was significantly reduced ($p < 0.05$), and the apoptosis rates of the EXOs group and the AS-IV group were also significantly reduced ($p < 0.05$). According to the results shown in Figure 2C–F, compared with the blank group, the AS-IV EXOs group's cell viability, cell state, adhesion number, and migration rate were significantly increased ($p < 0.05$). Therefore, the AS-IV EXOs had a significant improved impact on alleviating the damage of HUVECs under high glucose stimulation.

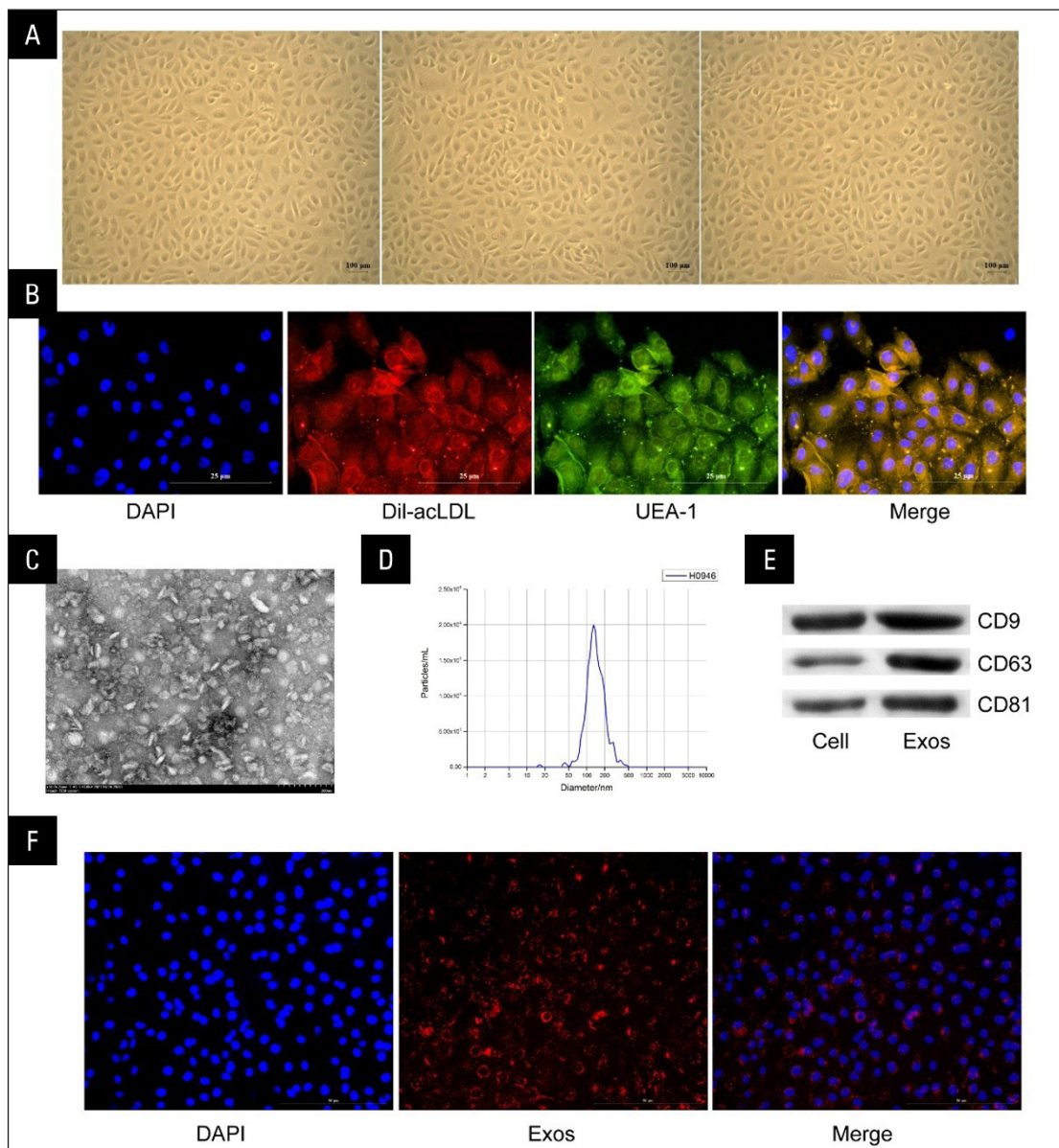


Figure 1. Absorption of astragaloside IV drug-loaded exosomes (AS-IV) Exos by inducing human umbilical vein endothelial cells (HUVECs). **A.** Photomicrographic image of endothelial progenitor cells (EPCs); **B.** Fluorescence microscopic images of EPCs; **C.** Transmission electron microscope (TEM) measurement of EPC-derived Exos. **D.** Nanoparticle tracking analysis (NTA) measurement of EPC-derived Exos; **E.** Western blot (WB) was performed to detect CD9, CD63, and CD81 levels; **F.** Fluorescence microscopic images of AS-IV Exos uptake by HUVECs

AS-IV EXOs promoted the tube formation of HUVECs and the expression of miR-214 under high glucose stimulation

According to Figure 3A, compared with the blank group, the number of tubes in the AS-IV EXOs group increased significantly ($p < 0.05$). From Figure 3B, compared with the blank group, the AS-IV EXOs group significantly increased the expression levels of Ang-1, PI3K, Akt, and Tie-2 ($p < 0.05$). From Figure 3C, compared with the blank group, the AS-IV EXOs group significantly increased the expression levels of Ang-1, p-PI3K, p-Akt, and Tie-2 ($p < 0.05$). From Figure 3D,

the expression of miR-214 in the AS-IV EXOs group also increased significantly compared with the AS-IV group and the EXOs group ($p < 0.05$). Hence, the AS-IV EXOs significantly promoted the tube formation of HUVECs and the expression of miR-214 under high glucose stimulation.

AS-IV EXOs promoted the formation of HUVECs by adjusting the level of miR-214

As shown in Figure 4A, the expression level of miR-214 mimic in the miR-214 group was significantly increased compared with the NC-mimic group ($p < 0.05$).

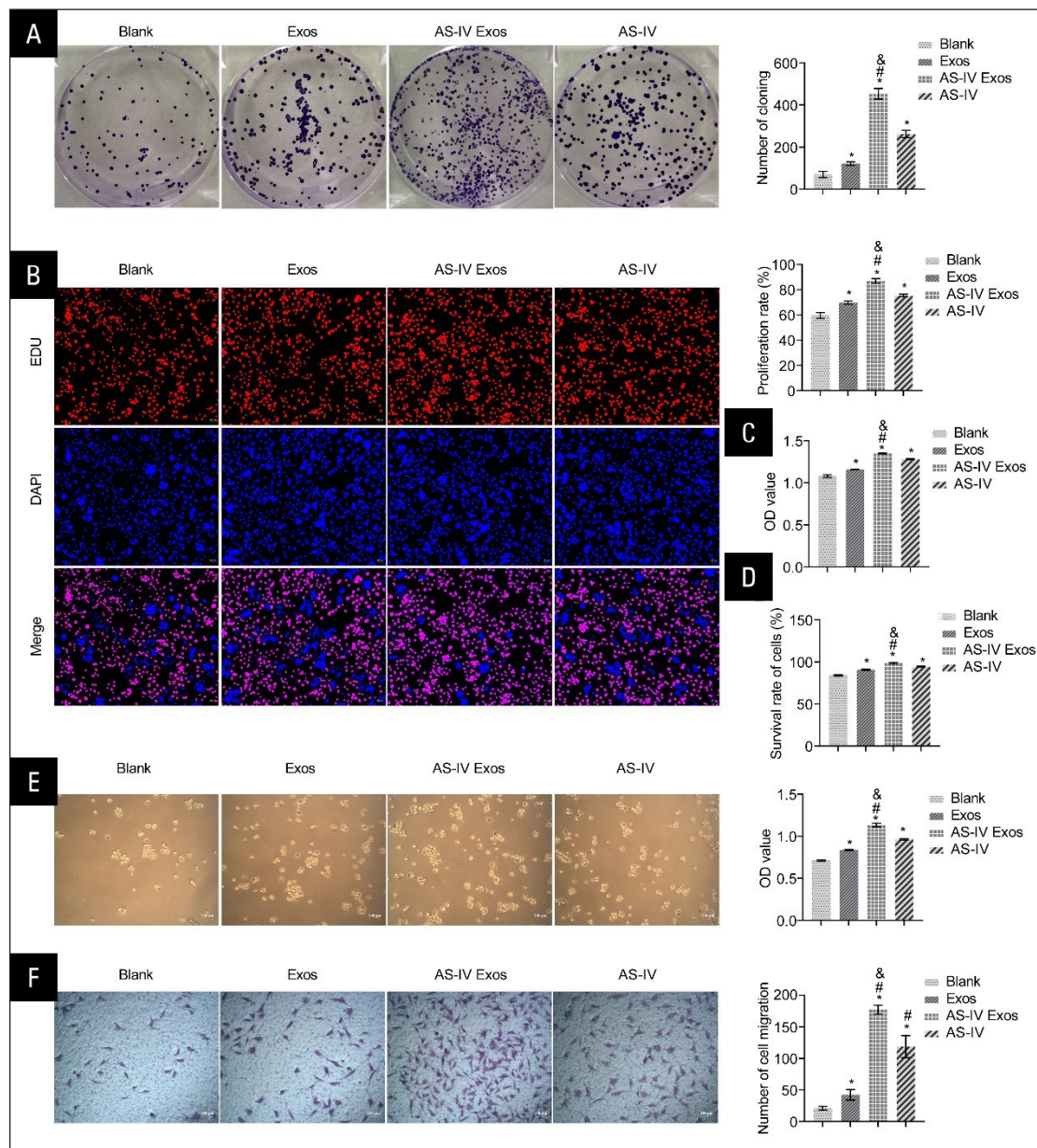


Figure 2. The effect of astragaloside IV drug-loaded exosomes (AS-IV Exos) on cell viability and tube formation of human umbilical vein endothelial cells (HUVECs) damaged by high glucose. **A.** Cell clone formation assay results; **B.** Ethylenediurea (EDU) was used to detect the apoptotic rate of HUVECs; **C.** CCK-8 assay was used to detect HUVECs proliferation; **D.** Trypan blue staining was used to measure cell viability; **E.** Cell adhesion was tested by adhesion assays; **F.** Transwell assays were used to evaluate HUVECs migration. * $p < 0.05$ vs. the blank group, # $p < 0.05$ vs. the Exos group, & $p < 0.05$ vs. the AS-IV group

At the same time, compared with the NC-inhibitor group, the expression level of miR-214 in the miR-214 inhibitor group was significantly decreased ($p < 0.05$). This indicated that the transfection of miR-214 was successful. Under the regulation of AS-IV EXOs, as shown in Figure 4B and 4C, compared with the miR-214 inhibitor group, the expression levels of vascular growth-related mRNA (*PI3K*, *Akt*, *Ang-1*, and *Tie-2*) and proteins (p-PI3K, p-Akt, Ang-1, and Tie-2) in the AS-IV EXOs + miR-214 inhibitor group increased significantly ($p < 0.05$), which indicated that AS-IV EXOs could reverse the inhibition of

downstream related genes caused by down-regulation of miR-214. As shown in Figure 4D, compared with the NC-mimic and NC-inhibitor groups, the number of tubes in the miR-214 mimic group and the miR-214 inhibitor group were significantly increased ($p < 0.05$). Compared with the miR-214 mimic and the miR-214 inhibitor groups, the AS-IV EXOs + miR-214 mimic and the AS-IV EXOs + miR-214 inhibitor group also had significant improvement ($p < 0.05$). This suggests that AS-IV EXOs can promote the angiogenesis HUVECs by regulating miR-214 levels.

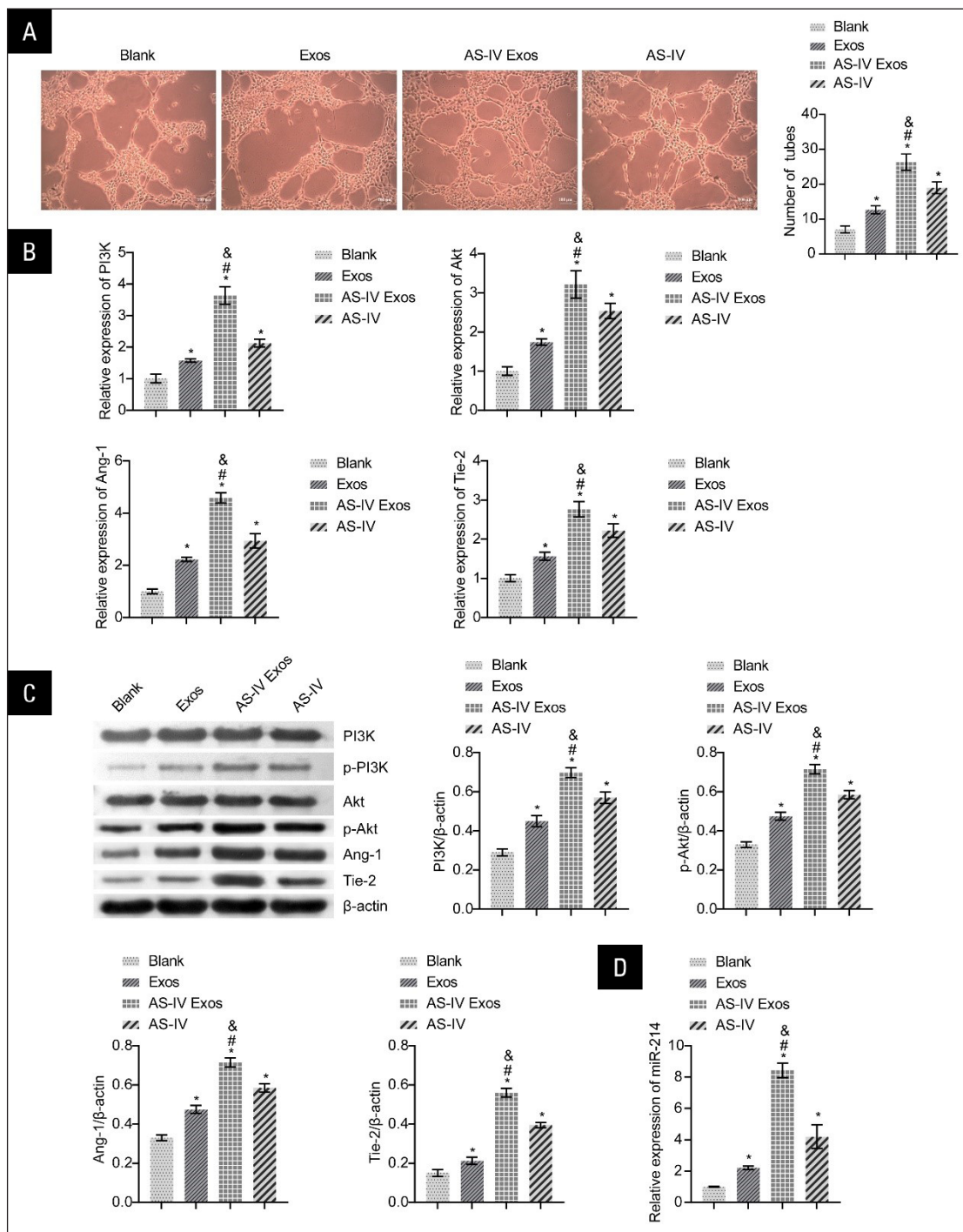


Figure 4. Astragaloside IV drug-loaded exosomes (AS-IV EXOs) promoted the formation of human umbilical vein endothelial cells (HUVECs) by adjusting the level of miR-214. (A). Quantitative real-time polymerase chain reaction (qRT-PCR) was used to assess the relative expressions of miR-214. (B). qRT-PCR was used to assess the angiogenesis-associated mRNA expressions of Ang-1, PI3K, p-PI3K, Akt, p-Akt, and Tie-2. (C). Western blot WB was used to measure the angiogenesis-associated protein expressions of PI3K, p-Akt, Ang-1, and Tie-2. (D). The number of tubes formed by HUVECs. NS — no significance, * $p < 0.05$

Discussion

An important marker of DM is vascular endothelial dysfunction after endothelial cell injury induced by hyperglycaemia [19, 20]. An active compound extracted from AS-IV can improve vascular endothelial dysfunction

caused by hyperglycaemia [21]. In order to improve the delivery efficiency of AS-IV, natural and efficient drug delivery system EXOs can also be considered [22, 23]. Our research results preliminarily suggest that AS-IV EXOs derived from EPCs can improve the viability and tube number of human endothelial cells damaged

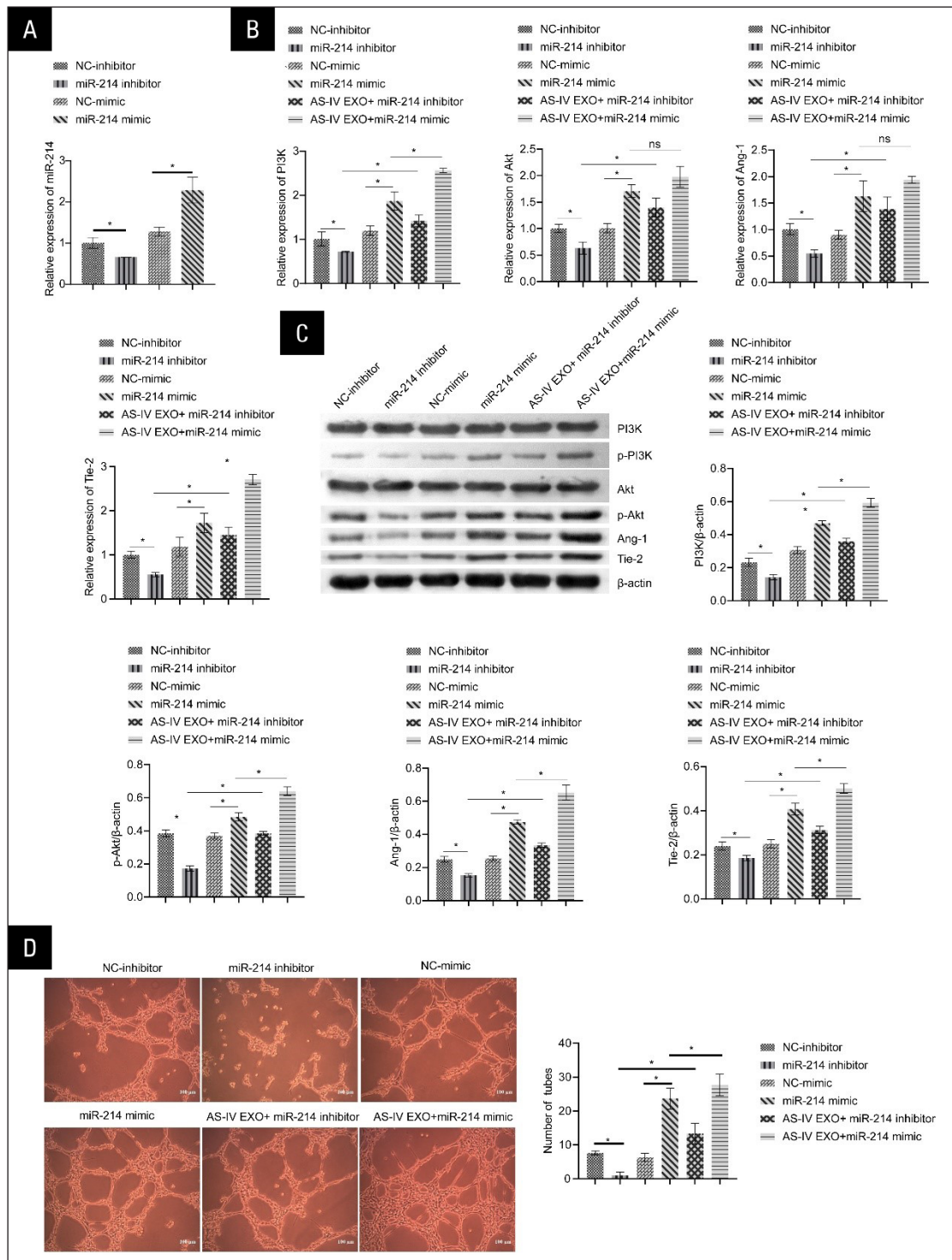


Figure 3. Astragaloside IV drug-loaded exosomes (AS-IV EXOs) promoted the tube formation of human umbilical vein endothelial cells (HUVECs) and the expression of miR-214 under high glucose stimulation. **A.** The number of tubes formed by HUVECs; **B.** Quantitative real-time polymerase chain reaction (qRT-PCR) was used to assess the relative expressions of Ang-1, PI3K, Akt, p-Akt, and Tie-2; **C.** Western blot was used to measure the expressions of Ang-1, PI3K, p-PI3K, p-Akt, and Tie-2; **D.** qRT-PCR was used to assess the relative expressions of miR-214. * $p < 0.05$ vs. the blank group, # $p < 0.05$ vs. the Exos group, &#pound; $p < 0.05$ vs. the AS-IV group

by high glucose. After transfecting the damaged cells with miR-214 inhibitor, it was found that AS-IV EXOs improved the cell damage recovery and its function by promoting the expression of miR-214.

DM is related to long-term damage, dysfunction, and failure of the eyes, kidneys, nerves, heart, and blood vessels. Symptoms of DM include polyuria, polydipsia, weight loss, blurred vision, and other symptoms. Acute

diabetes with features such as ketoacidosis can also be life-threatening [24, 25]. Under high glucose stimulation, aldose reductase will convert excess glucose into sorbitol and fructose, activate the corresponding signal pathway, oxidize NADPH to NADP⁺ and reduce NAD⁺ to NADH, intensify the glycolysis process, and promote the synthesis of DAG. With the activation of protein kinase C and the increase in the ratio of NADH/NAD⁺, it will eventually lead to endothelial dysfunction [24].

There are various treatments for the endothelial injury caused by DM, including empagliflozin on top of metformin [26], adiponectin [27], diet [28], and exercise [29]. We tried to load the drug AS-IV on EXOs. The results showed that it could restore endothelial cell damage under high glucose stimulation, which provides a reference for the diversified treatment of endothelial system damage caused by DM.

We found that AS-IV EXOs improved endothelial cell damage repair and function by promoting miR-214 expression. The results of Qu Nie et al. and Yuyan Fan et al. showed that oral administration of AS-IV could increase the production of NO and the expression of eNOS, and significantly improve the endothelial dysfunction of rat thoracic aorta and glomerular cells, respectively [8, 30]. Bin Leng et al. also found that AS-IV saved the endothelial dysfunction induced by high glucose by restraining the P2X7R-dependent P38 MAPK signalling pathway [9]. Because miR-214 can inhibit endothelial cell senescence and induce angiogenesis [31], the overexpression of eNOS can also improve endothelial dysfunction [8, 30]. Still, AS-IV EXOs promotes the expression of miR-214 and eNOS, clarifying the relationship between the two, and the exact target of miR-214 can be used as a future research direction.

Conclusions

In summary, AS-IV EXOs derived from EPCs can improve the viability and tube formation of human endothelial cells damaged by high glucose by promoting the expression of miR-214. This discovery provides a theoretical basis for a better understanding of the regulatory direction of AS-IV EXOs in endothelial cells damaged by high glucose.

Conflict of interest

The authors declare that they have no conflict of interest regarding this work.

Acknowledgements

This work was supported by Scientific Research Project of Hunan Provincial Health Commission (20201388). This work was supported by National Natural Science Foundation of China Youth Science Fund Project (81904217).

Authors' contributions

X.Z. and H.X. participated in the conceptualization work, formal analysis, methodology, writing-original draft and writing-review, and editing. X.B., Y.Z., W.H., Y.L., and C.Z. participated in the analysed data, data curation, and writing the original draft. X.L. and W.X. participated in the project administration, funding acquisition, and writing-review and editing. The authors declare that all data were generated in-house and that no paper mill was used. All authors read and approved the manuscript in its present form.

References

- Galicía-García U, Benito-Vicente A, Jebari S, et al. Pathophysiology of Type 2 Diabetes Mellitus. *Int J Mol Sci.* 2020; 21(17), doi: [10.3390/ijms21176275](https://doi.org/10.3390/ijms21176275), indexed in Pubmed: [32872570](https://pubmed.ncbi.nlm.nih.gov/32872570/).
- Niu C, Chen Z, Kim KT, et al. Metformin alleviates hyperglycemia-induced endothelial impairment by downregulating autophagy via the Hedgehog pathway. *Autophagy.* 2019; 15(5): 843–870, doi: [10.1080/15548627.2019.1569913](https://doi.org/10.1080/15548627.2019.1569913), indexed in Pubmed: [30653446](https://pubmed.ncbi.nlm.nih.gov/30653446/).
- Cho NH, Shaw JE, Karuranga S, et al. IDF Diabetes Atlas: Global estimates of diabetes prevalence for 2017 and projections for 2045. *Diabetes Res Clin Pract.* 2018; 138: 271–281, doi: [10.1016/j.diabres.2018.02.023](https://doi.org/10.1016/j.diabres.2018.02.023), indexed in Pubmed: [29496507](https://pubmed.ncbi.nlm.nih.gov/29496507/).
- Cole JB, Florez JC. Genetics of diabetes mellitus and diabetes complications. *Nat Rev Nephrol.* 2020; 16(7): 377–390, doi: [10.1038/s41581-020-0278-5](https://doi.org/10.1038/s41581-020-0278-5), indexed in Pubmed: [32398868](https://pubmed.ncbi.nlm.nih.gov/32398868/).
- Liu J, Jiang C, Ma Xu, et al. Notoginsenoside Fc Accelerates Reendothelialization following Vascular Injury in Diabetic Rats by Promoting Endothelial Cell Autophagy. *J Diabetes Res.* 2019; 2019: 9696521, doi: [10.1155/2019/9696521](https://doi.org/10.1155/2019/9696521), indexed in Pubmed: [31565658](https://pubmed.ncbi.nlm.nih.gov/31565658/).
- Knapp M, Tu X, Wu R. Vascular endothelial dysfunction, a major mediator in diabetic cardiomyopathy. *Acta Pharmacol Sin.* 2019; 40(1): 1–8, doi: [10.1038/s41401-018-0042-6](https://doi.org/10.1038/s41401-018-0042-6), indexed in Pubmed: [29867137](https://pubmed.ncbi.nlm.nih.gov/29867137/).
- Liu X, Shang S, Chu W, et al. Astragaloside IV ameliorates radiation-induced senescence via antioxidative mechanism. *J Pharm Pharmacol.* 2020; 72(8): 1110–1118, doi: [10.1111/jphp.13284](https://doi.org/10.1111/jphp.13284), indexed in Pubmed: [32412100](https://pubmed.ncbi.nlm.nih.gov/32412100/).
- Nie Qu, Zhu L, Zhang L, et al. Astragaloside IV protects against hyperglycemia-induced vascular endothelial dysfunction by inhibiting oxidative stress and Calpain-1 activation. *Life Sci.* 2019; 232: 116662, doi: [10.1016/j.lfs.2019.116662](https://doi.org/10.1016/j.lfs.2019.116662), indexed in Pubmed: [31323271](https://pubmed.ncbi.nlm.nih.gov/31323271/).
- Leng B, Li C, Sun Y, et al. Protective Effect of Astragaloside IV on High Glucose-Induced Endothelial Dysfunction via Inhibition of P2X7R Dependent P38 MAPK Signaling Pathway. *Oxid Med Cell Longev.* 2020; 2020: 5070415, doi: [10.1155/2020/5070415](https://doi.org/10.1155/2020/5070415), indexed in Pubmed: [33014270](https://pubmed.ncbi.nlm.nih.gov/33014270/).
- Zhang L, Yu D. Exosomes in cancer development, metastasis, and immunity. *Biochim Biophys Acta Rev Cancer.* 2019; 1871(2): 455–468, doi: [10.1016/j.bbcan.2019.04.004](https://doi.org/10.1016/j.bbcan.2019.04.004), indexed in Pubmed: [31047959](https://pubmed.ncbi.nlm.nih.gov/31047959/).
- Betzer O, Perets N, Angel A, et al. In Vivo Neuroimaging of Exosomes Using Gold Nanoparticles. *ACS Nano.* 2017; 11(11): 10883–10893, doi: [10.1021/acsnano.7b04495](https://doi.org/10.1021/acsnano.7b04495), indexed in Pubmed: [28960957](https://pubmed.ncbi.nlm.nih.gov/28960957/).
- Barile L, Lionetti V, Cervio E, et al. Extracellular vesicles from human cardiac progenitor cells inhibit cardiomyocyte apoptosis and improve cardiac function after myocardial infarction. *Cardiovasc Res.* 2014; 103(4): 530–541, doi: [10.1093/cvr/cvu167](https://doi.org/10.1093/cvr/cvu167), indexed in Pubmed: [25016614](https://pubmed.ncbi.nlm.nih.gov/25016614/).
- Johnson TK, Zhao L, Zhu D, et al. Exosomes derived from induced vascular progenitor cells promote angiogenesis in vitro and in an in vivo rat hindlimb ischemia model. *Am J Physiol Heart Circ Physiol.* 2019; 317(4): H765–H776, doi: [10.1152/ajpheart.00247.2019](https://doi.org/10.1152/ajpheart.00247.2019), indexed in Pubmed: [31418583](https://pubmed.ncbi.nlm.nih.gov/31418583/).
- Barile L, Vassalli G. Exosomes: Therapy delivery tools and biomarkers of diseases. *Pharmacol Ther.* 2017; 174: 63–78, doi: [10.1016/j.pharmthera.2017.02.020](https://doi.org/10.1016/j.pharmthera.2017.02.020), indexed in Pubmed: [28202367](https://pubmed.ncbi.nlm.nih.gov/28202367/).
- Luzi E, Marini F, Sala SC, et al. Osteogenic differentiation of human adipose tissue-derived stem cells is modulated by the miR-26a targeting of the SMAD1 transcription factor. *J Bone Miner Res.* 2008; 23(2): 287–295, doi: [10.1359/jbmr.071011](https://doi.org/10.1359/jbmr.071011), indexed in Pubmed: [18197755](https://pubmed.ncbi.nlm.nih.gov/18197755/).
- Yang B, Li S, Zhu J, et al. miR-214 Protects Against Uric Acid-Induced Endothelial Cell Apoptosis. *Front Med (Lausanne).* 2020; 7: 411, doi: [10.3389/fmed.2020.00411](https://doi.org/10.3389/fmed.2020.00411), indexed in Pubmed: [32850909](https://pubmed.ncbi.nlm.nih.gov/32850909/).
- Li S, Xie Y, Yang B, et al. MicroRNA-214 targets COX-2 to antagonize indoxyl sulfate (IS)-induced endothelial cell apoptosis. *Apoptosis.* 2020; 25(1-2): 92–104, doi: [10.1007/s10495-019-01582-4](https://doi.org/10.1007/s10495-019-01582-4), indexed in Pubmed: [31820187](https://pubmed.ncbi.nlm.nih.gov/31820187/).
- Xiao P, Zhu Xu, Sun J, et al. Cartilage tissue miR-214-3p regulates the TrkB/ShcB pathway paracrine VEGF to promote endothelial cell migration and angiogenesis. *Bone.* 2021; 151: 116034, doi: [10.1016/j.bone.2021.116034](https://doi.org/10.1016/j.bone.2021.116034), indexed in Pubmed: [34107348](https://pubmed.ncbi.nlm.nih.gov/34107348/).

19. La Sala L, Prattichizzo F, Ceriello A. The link between diabetes and atherosclerosis. *Eur J Prev Cardiol.* 2019; 26(2_suppl): 15–24, doi: [10.1177/2047487319878373](https://doi.org/10.1177/2047487319878373), indexed in Pubmed: [31722564](https://pubmed.ncbi.nlm.nih.gov/31722564/).
20. Erener S. Diabetes, infection risk and COVID-19. *Mol Metab.* 2020; 39: 101044, doi: [10.1016/j.molmet.2020.101044](https://doi.org/10.1016/j.molmet.2020.101044), indexed in Pubmed: [32585364](https://pubmed.ncbi.nlm.nih.gov/32585364/).
21. Leng B, Tang F, Lu M, et al. Astragaloside IV improves vascular endothelial dysfunction by inhibiting the TLR4/NF- κ B signaling pathway. *Life Sci.* 2018; 209: 111–121, doi: [10.1016/j.lfs.2018.07.053](https://doi.org/10.1016/j.lfs.2018.07.053), indexed in Pubmed: [30081006](https://pubmed.ncbi.nlm.nih.gov/30081006/).
22. Mehryab F, Rabbani S, Shahhosseini S, et al. Exosomes as a next-generation drug delivery system: An update on drug loading approaches, characterization, and clinical application challenges. *Acta Biomater.* 2020; 113: 42–62, doi: [10.1016/j.actbio.2020.06.036](https://doi.org/10.1016/j.actbio.2020.06.036), indexed in Pubmed: [32622055](https://pubmed.ncbi.nlm.nih.gov/32622055/).
23. Ha DH, Kim HK, Lee J, et al. Mesenchymal Stem/Stromal Cell-Derived Exosomes for Immunomodulatory Therapeutics and Skin Regeneration. *Cells.* 2020; 9(5), doi: [10.3390/cells9051157](https://doi.org/10.3390/cells9051157), indexed in Pubmed: [32392899](https://pubmed.ncbi.nlm.nih.gov/32392899/).
24. American Diabetes Association. Diagnosis and classification of diabetes mellitus. *Diabetes Care.* 2013; 36 Suppl 1: S67–S74, doi: [10.2337/dc13-S067](https://doi.org/10.2337/dc13-S067), indexed in Pubmed: [23264425](https://pubmed.ncbi.nlm.nih.gov/23264425/).
25. Nägele MP, Haubner B, Tanner FC, et al. Endothelial dysfunction in COVID-19: Current findings and therapeutic implications. *Atherosclerosis.* 2020; 314: 58–62, doi: [10.1016/j.atherosclerosis.2020.10.014](https://doi.org/10.1016/j.atherosclerosis.2020.10.014), indexed in Pubmed: [33161318](https://pubmed.ncbi.nlm.nih.gov/33161318/).
26. Lunder M, Janić M, Japelj M, et al. Empagliflozin on top of metformin treatment improves arterial function in patients with type 1 diabetes mellitus. *Cardiovasc Diabetol.* 2018; 17(1): 153, doi: [10.1186/s12933-018-0797-6](https://doi.org/10.1186/s12933-018-0797-6), indexed in Pubmed: [30509271](https://pubmed.ncbi.nlm.nih.gov/30509271/).
27. Achari AE, Jain SK. Adiponectin, a Therapeutic Target for Obesity, Diabetes, and Endothelial Dysfunction. *Int J Mol Sci.* 2017; 18(6), doi: [10.3390/ijms18061321](https://doi.org/10.3390/ijms18061321), indexed in Pubmed: [28635626](https://pubmed.ncbi.nlm.nih.gov/28635626/).
28. Torres-Peña JD, García-Ríos A, Delgado-Casado N, et al. Mediterranean diet improves endothelial function in patients with diabetes and prediabetes: A report from the CORDIOPREV study. *Atherosclerosis.* 2018; 269: 50–56, doi: [10.1016/j.atherosclerosis.2017.12.012](https://doi.org/10.1016/j.atherosclerosis.2017.12.012), indexed in Pubmed: [29274507](https://pubmed.ncbi.nlm.nih.gov/29274507/).
29. Qiu S, Cai X, Yin H, et al. Impact of walking on glycemic control and other cardiovascular risk factors in type 2 diabetes: a meta-analysis. *PLoS One.* 2014; 9(10): e109767, doi: [10.1371/journal.pone.0109767](https://doi.org/10.1371/journal.pone.0109767), indexed in Pubmed: [25329391](https://pubmed.ncbi.nlm.nih.gov/25329391/).
30. Fan Y, Fan H, Zhu B, et al. Astragaloside IV protects against diabetic nephropathy via activating eNOS in streptozotocin diabetes-induced rats. *BMC Complement Altern Med.* 2019; 19(1): 355, doi: [10.1186/s12906-019-2728-9](https://doi.org/10.1186/s12906-019-2728-9), indexed in Pubmed: [31805910](https://pubmed.ncbi.nlm.nih.gov/31805910/).
31. van Balkom BWM, de Jong OG, Smits M, et al. Endothelial cells require miR-214 to secrete exosomes that suppress senescence and induce angiogenesis in human and mouse endothelial cells. *Blood.* 2013; 121(19): 3997–4006, S1, doi: [10.1182/blood-2013-02-478925](https://doi.org/10.1182/blood-2013-02-478925), indexed in Pubmed: [23532734](https://pubmed.ncbi.nlm.nih.gov/23532734/).